Molecular Therapy
Nucleic Acids
Original Article

# Antisense Oligonucleotide-Mediated Terminal Intron Retention of the *SMN2* Transcript

Loren L. Flynn,[1,2,4] Chalermchai Mitrpant,[2,3,4] Ianthe L. Pitout,[1,2] Sue Fletcher,[1,2] and Steve D. Wilton[1,2]

[1]Centre for Comparative Genomics, Murdoch University, Perth, WA, Australia; [2]Perron Institute for Neurological and Translational Science, Perth, WA, Australia; [3]Department of Biochemistry, Mahidol University, Bangkok, Thailand

**The severe childhood disease spinal muscular atrophy (SMA) arises from the homozygous loss of the survival motor neuron 1 gene (*SMN1*). A homologous gene potentially encoding an identical protein, *SMN2* can partially compensate for the loss of *SMN1*; however, the exclusion of a critical exon in the coding region during mRNA maturation results in insufficient levels of functional protein. The rate of transcription is known to influence the alternative splicing of gene transcripts, with a fast transcription rate correlating to an increase in alternative splicing. Conversely, a slower transcription rate is more likely to result in the inclusion of all exons in the transcript. Targeting *SMN2* with antisense oligonucleotides to influence the processing of terminal exon 8 could be a way to slow transcription and induce the inclusion of exon 7. Interestingly, following oligomer treatment of SMA patient fibroblasts, we observed the inclusion of exon 7, as well as intron 7, in the transcript. Because the normal termination codon is located in exon 7, this exon/intron 7-*SMN2* transcript should encode the normal protein and only carry a longer 3′ UTR. Further studies showed the extra 3′ UTR length contained a number of regulatory motifs that modify transcript and protein regulation, leading to translational repression of SMN. Although unlikely to provide therapeutic benefit for SMA patients, this novel technique for gene regulation could provide another avenue for the repression of undesirable gene expression in a variety of other diseases.**

## INTRODUCTION

With a frequency of 1 in 10,000 live births,[1] the neurodegenerative disease spinal muscular atrophy (SMA) is the leading genetic cause of infant death.[2] SMA arises from inadequate levels of the survival motor neuron (SMN) protein that ultimately results in the death of motor neurons. While the survival motor neuron 1 (*SMN1*) gene is missing in most SMA patients, copies of the homologous gene, *SMN2*, potentially compensate for SMN production[3]; however, a C > T base change in *SMN2* exon 7 results in exclusion of the exon from 90% of neuronal *SMN2* transcripts.[3,4] To date, the main RNA therapeutic focus for SMA has been the use of antisense oligonucleotides (AOs) to enhance *SMN2* exon 7 inclusion and increase SMN levels (for review, see Porensky and Burghes[5]). In particular, a 2′O-methoxyethyl (MOE) AO covering the ISS-N1 splicing domain (*Anti-ISS-N1*) has shown promise in clinical trials[6–8] and has recently received approval by the U.S. Food and Drug Administration.[9] However, the therapy is by no means definitive, with unknown consequences of long-term AO exposure and further improvements in AO efficacy needed before this therapy can be considered a qualified success. While other studies have focused on targeting AOs to intronic splice silencing motifs to enhance exon 7 inclusion,[8,10–12] AO-mediated splice modification has broader potential.

The strategy described here was focused on targeting AOs to the last exon in an attempt to slow transcription rates and concurrent pre-mRNA processing to temporarily stall the spliceosome machinery. Others have shown that a slow RNA polymerase II elongation rate during transcription can increase the "window of opportunity" for upstream splicing events, with alternative exons more likely to be included in the mature transcript.[13,14] To determine whether slower transcription elongation could be induced by an AO, we targeted AOs to *SMN2* exon 8 in an attempt to increase the inclusion of *SMN2* exon 7 in the transcript.

Unexpectedly, AOs targeting *SMN2* exon 8 induced the retention of exon 7 and intron 7 in the mature transcript. Interestingly, an AO covering the exon 8 acceptor site has been reported by others to induce exon 7 and intron 7 retention, yet this work was not pursued further.[15] Because the normal termination codon is located within exon 7, this induced transcript should therefore encode the normal full-length protein; however, the size of the 3′ UTR is increased. It is well documented that the length of the 3′ UTR can affect transcript stability and protein translation, with longer 3′ UTRs having more opportunity for the binding of microRNAs and regulatory elements (for review, see Barrett et al.[16]). However, the consequences of intron retention within the mature transcript, and more specifically within the 3′ UTRs, are a more recently explored and less well understood area.

A study by Braunschweig and colleagues[17] reported that three-quarters of mammalian multi-exon genes exhibit intron retention within

Received 20 December 2017; accepted 25 January 2018;
https://doi.org/10.1016/j.omtn.2018.01.011.

[4]These authors contributed equally to this work.

**Correspondence:** Steve D. Wilton, Centre for Comparative Genomics, Health Research Centre, Building 390, Murdoch University, 90 South Street, Perth, WA 6150, Australia.
**E-mail:** swilton@ccg.murdoch.edu.au

the mature transcript as a result of alternative splicing events. While 6%–16% of 3′ UTRs are suggested to contain introns,[18] it is unclear at this stage what percentage of these have the propensity to retain an intron within the mature message. While transcripts containing introns within the 3′ UTR were once believed to be non-functional due to nonsense-mediated decay,[19,20] there is now evidence to show that intron retention within the mature message is an important mechanism for transcript and protein regulation (for review, see Bicknell et al.[18] and Ge and Porse[20]). Tissue-specific transcript regulation by intron retention is particularly common in neuronal cells during differentiation and maturity,[21] and recent studies have revealed a role for intron retention in hematopoietic cellular differentiation.[22] Furthermore, intron retention within the 3′ UTR has been shown to play a role in transcript autoregulation to maintain protein homeostasis, a mechanism that is particularly common in proteins involved in forming the spliceosome and in regulating pre-mRNA processing.[23,24]

A number of factors have been reported to regulate splicing events resulting in intron retention, with a correlation observed between intron retention and the presence of certain regulatory *cis* elements.[17] Of particular interest, intron retention has been suggested to be the result of stalling of the RNA polymerase II elongation due to poor splicing factor recruitment and weakened splicing in non-essential transcripts.[17,25] Other factors influencing this mechanism include the position of the intron within the transcript, reduced intron length, an increase in G/C content within the intron, and weak splice site strength.[17]

While factors that determine intron retention have been studied in canonical splicing events, it is unknown what role they play in mediating AO-induced intron retention and transcript expression. Consequently, this study focused on gaining a further understanding of the mechanisms influencing AO-induced intron retention and, furthermore, investigating how it can impact transcript and protein expression as a potential strategy in treating genetic disease.

## RESULTS

### Targeting AOs to Exon 8 Results in Exon 7 and Intron 7 Retention in *SMN2* Transcripts

SMA type I fibroblasts (Coriell GM03813) were transfected with 2′O-methyl AOs targeting *SMN2* exon 8 (for binding coordinates and AO sequences, see Table 3) at 300, 150, and 75 nM and incubated (37°C) for 48 hr. RT-PCR analysis (Figure 1A) of *SMN2* showed an increase in abundance of an approximately 850-bp product, which was confirmed by sequencing (Figure 1B) to be the *SMN2* transcript retaining exon 7, as well as intron 7 (848 bp). This product is referred to as exon/intron 7-*SMN2* and is labeled ex/in7 in the figures. Because the stop codon is located within exon 7, the addition of an extra 444-bp intronic sequence should encode the same protein as *SMN1*, but increases the length of the 3′ UTR (Figure 1C). These results were reproducible in two unrelated SMA patient primary cell strains (data not shown), including an SMA type II patient (prepared in-house) and an SMA type I patient with only one copy of *SMN2* (Coriell GM00232). Two additional bands were observed at approximately 100 bp above and 100 bp below the exon/intron 7-*SMN2* transcript. The larger band was deemed to be a PCR artifact because it was unable to be re-amplified and disappeared following increasing primer annealing temperature. The lower band was confirmed by sequencing to be the naturally occurring Δ5-*SMN2* transcript containing intron 7 (data not shown).

The initial screening of AO sequences 1–18 is shown in Figure S1. Following preliminary screening, additional AOs were designed by microwalking around promising AO target sites, shifting up or downstream of the original sites (Table 3). Analysis of *SMN2* transcripts following transfection with refined AO sequences showed an improvement in AO-induced exon/intron 7 retention (Figure 1A). A clear dose response was observed in all AO-treated cells, with AOs 10, 18, 24, and 25 consistently inducing the highest levels of inclusion across experiments (n = 6). These promising AOs were therefore selected for further evaluation, including protein analysis.

### Splice Site Analysis Shows a Weak Exon 7 Donor Splice Site

To further investigate the exon/intron 7-*SMN2* transcript induced by AOs targeting exon 8, we analyzed splice site scores (Table 1) using the online Human Splicing Finder 3.0 website.[26] *SMN2* exon 7 was predicted to have a very strong acceptor site with a score of 98.2 out of a possible 100, while the donor splice site was weaker, scoring 82.81 out of 100. The exon 8 acceptor splice site had a predicted score of 91.9 out of 100. While these splice site scores are only a predicted measurement of the likelihood of the site being recognized by the splicing machinery, the comparatively weaker exon 7 donor splice site could lead to reduced splicing at the exon/intron 7 junction when the intron 7/exon 8 junction is further compromised following AO treatment.

### PMO Delivery by Electroporation Improves Exon/Intron 7 Inclusion, Inducing a Decrease in SMN Protein

Previously identified optimal 2′O-methyl AO sequences 10, 18, 24, and 25 were resynthesized as phosphorodiamidate morpholino oligomers (PMOs) by Genetools (Philomath, OR, USA), and are now cited as PMOs 10, 18, 24, and 25. PMOs were administered to cells using nucleofection for optimal delivery at 1 and 0.5 μM for SMN transcript and protein analysis by RT-PCR and western blot, respectively. Nucleofection of PMOs showed increased levels of exon/intron 7 retention in the mature transcript compared with the same sequences tested as 2′O-methyl AOs, with a clear reduction in the levels of FL-*SMN* and Δ7-*SMN* transcripts. In particular, PMO-10 induced almost 100% exon/intron 7 inclusion as determined by RT-PCR (Figure 2A).

Interestingly, western blot analysis of SMN protein levels revealed a significant decrease in the amount of SMN detected in samples transfected with exon-8-targeting PMOs (Figures 2B and 2C). PMO-10 and PMO-24 were the most effective compounds inducing a respective 50% ($p = 0.022$) and 33% ($p = 0.027$) decrease in SMN protein when compared with the level observed in untreated fibroblasts

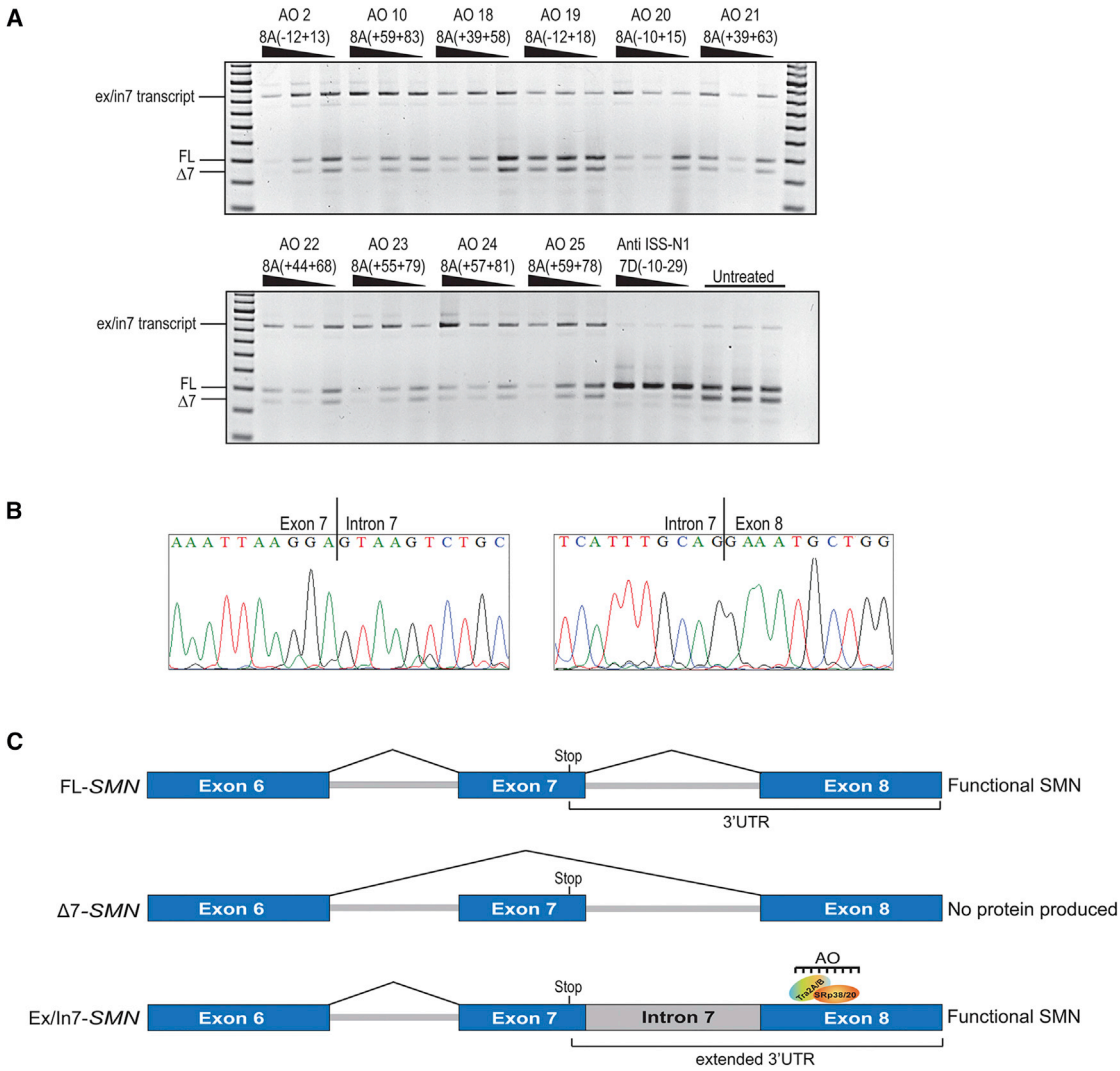


**Figure 1. *SMN* Transcript Analysis following 2′OMethyl AO Transfection**

Analysis of SMA fibroblasts following transfection with exon 8 targeting 2′O-methyl AOs, showing (A) RT-PCR analysis of *SMN2* transcripts from transfected fibroblasts (300, 150, 75 nM). *Anti-ISS-N1* was used as a positive control for transfection efficiency, and a sham control AO was used as a transfection negative control. A 100-bp marker was used for comparison, and an RT-PCR no-template negative control was loaded in the final lane, (B) sequencing chromatogram across *SMN2* exon 7 to intron 7 and intron 7 to exon 8, confirming the presence of intron 7 within the mature transcript, and (C) schematic showing *SMN2* transcripts identified within fibroblasts transfected with exon-8-targeting AOs, including full-length *SMN* (FL-*SMN*), the Δ7-*SMN* transcript missing exon 7, and the exon/intron 7 retained transcript (ex/in7-*SMN*) with the extended 3′ UTR.

(n = 4). The *Anti-ISS-N1* PMO sequence was transfected as a positive control and was shown to increase SMN levels by up to 80% compared with that in untreated SMA patient fibroblasts (p = 0.032).

### PMO-Induced SMN Knockdown Is Reproducible in Unaffected Fibroblasts

PMO-24 and PMO-25 were evaluated in non-SMA fibroblasts to determine the effects of intron 7 retention on SMN protein levels in cells with a higher baseline of SMN. PMOs were transfected by nucleofection at 1 and 0.5 μM, and incubated for 3 days prior to western blot analysis. RT-PCR analysis of the total *SMN* transcripts confirmed that exon-8-targeting AOs induce almost 100% exon/intron 7 retention, and hence this must represent both the *SMN1* and the *SMN2* transcripts (Figure 3A). Consistent with the findings in SMA patient fibroblasts, western blot analysis (Figures 3B and 3C) demonstrated that PMO-24 and PMO-25 effectively decreased the levels of SMN protein in non-SMA fibroblasts by 55% (p = 0.041) and 38% (p = 0.072), respectively (n = 3). *Anti-ISS-N1* was transfected as a positive control and was shown to increase the levels of SMN protein by up to 35% as seen in non-SMA cells transfected with the low AO dose; however, this was not statistically significant. Furthermore, an AO designed to induce exon 7 skipping was transfected into non-SMA fibroblasts as a positive control for downregulating SMN levels. Fibroblasts transfected with this PMO show a 76% decrease

**Table 1. Exons 7 and 8 Splice Site Predictions Using Human Splicing Finder 3.0**

| Exon | Splice Site Type | Splice Site Motif | Consensus Value (0–100) |
|---|---|---|---|
| 7 | acceptor | ttttccttacagGG | 98.2 |
| 7 | donor | GGAgtaagt | 82.81 |
| 8 | acceptor | tctcatttgcagGA | 91.9 |

in SMN levels compared with sham control and untreated fibroblasts ($p = 0.030$).

Functional SMN protein forms aggregates with the gemin proteins that fluoresce as bright sparkling foci, reminiscent of gems after antibody staining. Therefore, the presence of gems within the cell indicates functional localization of SMN protein. The percentages of fibroblast nuclei staining positive for gems were counted (Figure 4A). PMOs 10, 18, 24, and 25 were all transfected into non-SMA cells by nucleofection at 1 μM and incubated for 3 days prior to fixation and immunofluorescent staining. Interestingly, the sham control PMO induced an increase in nuclei containing gems from 16.3% in untreated fibroblasts to 20.6% following control AO transfection. However, PMOs 10, 18, 24, and 25 all decreased the number of nuclei containing gems, with as low as 7.3% of fibroblasts containing gems following transfection with PMO-10. In comparison, 25.9% of fibroblasts transfected with the *Anti-ISS-N1* PMO sequence express gems, while only 3.3% of those transfected with the exon skipping control PMO express gems. Representative images of fibroblasts transfected with each PMO are shown in Figure 4B.

PMOs targeting exon 8 induce more efficient retention of exon and intron 7 in both the *SMN1* and the *SMN2* transcripts compared with the 2′O-methyl AOs of the same sequence, and analysis of the SMN protein by western blot and immunofluorescence shows a further decrease in SMN expression following transfection. While the exon/intron 7-*SMN* transcript occurs naturally at low levels in untransfected cells, it appears that the extended 3′ UTR introduces a number of new regulatory mechanisms into the transcript that negatively impact on protein expression.

### Intron Retention Introduces Negative Regulatory Elements to the 3′ UTR

*In silico* analysis of the extended 3′ UTR was carried out using the online tools UTRscan,[27] miRBase,[28] Polyadq,[29] and DNA Functional Site Miner (DNA FS Miner).[30] Table 2 lists the potential regulatory elements identified within intron 7 from each of these databases,

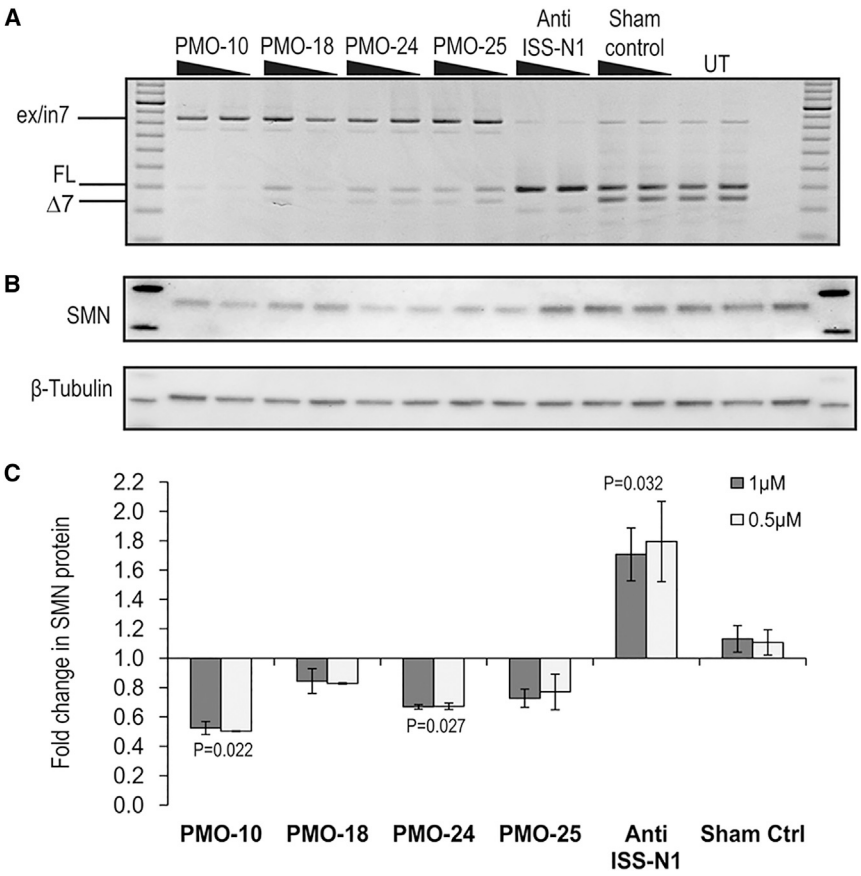


**Figure 2. *SMN* Transcript and Protein Analysis in SMA Fibroblasts following PMO Nucleofection**

*SMN* transcript and protein levels in SMA fibroblasts transfected with PMOs by nucleofection at 1 and 0.5 μM, showing (A) RT-PCR analysis of *SMN2* products confirming exon/intron retention, (B) western blots showing SMN protein levels compared with β-tubulin levels, and (C) densitometric analysis showing changes in SMN protein levels normalized against β-tubulin. SMN levels in transfected fibroblasts are shown as an n-fold change compared with those in samples from untreated cells. Error bars represent the SEM.

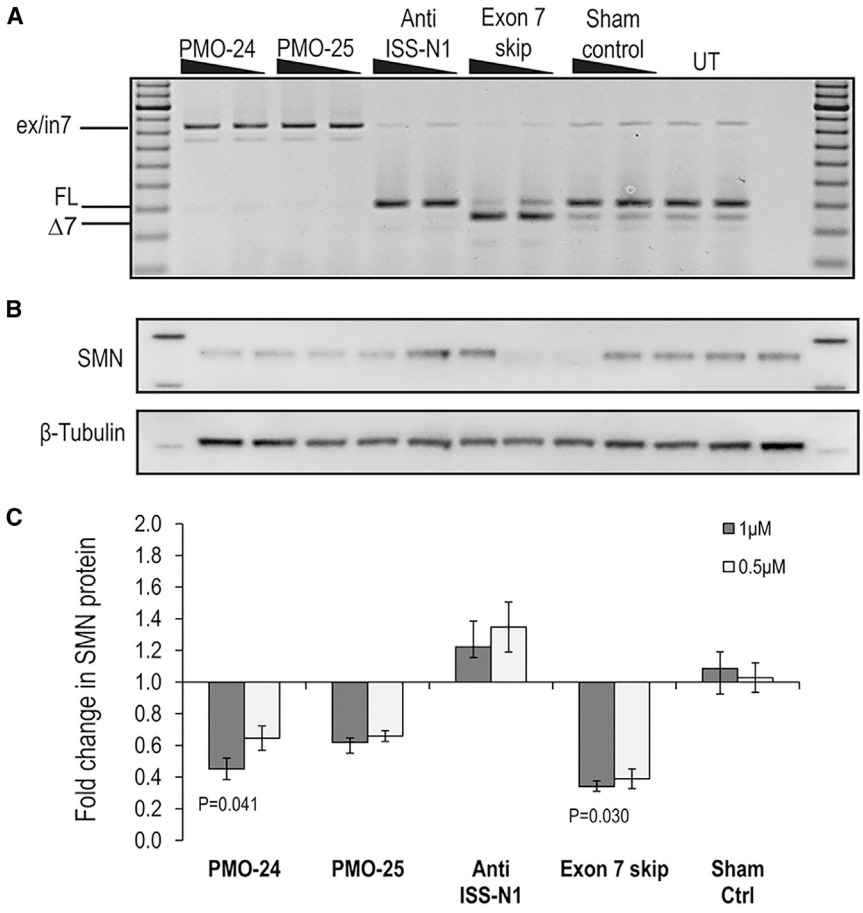


**Figure 3. *SMN* Transcript and Protein Analysis in Unaffected Fibroblasts following PMO Nucleofection**

*SMN* transcript and protein levels in unaffected fibroblasts transfected with PMOs by nucleofection at 1 and 0.5 μM, showing (A) RT-PCR analysis of *SMN* products confirming exon/intron retention, (B) western blots showing SMN protein levels compared with β-tubulin levels, and (C) densitometric analysis showing changes in SMN protein levels normalized against β-tubulin. SMN levels in transfected fibroblasts are shown as an n-fold change compared with those in samples from untreated cells. Error bars represent the SEM.

and Figure 5A illustrates the location of these elements within intron 7. *In silico* analysis of the extended 3′ UTR by the online tool UTRscan drew attention to two possible regulatory motifs known as the bearded (BRD) box and the K box. Each of these motifs has been shown by others to disrupt translation of neuronal gene transcripts during *Drosophila* development by recruiting microRNAs.[31,32] The BRD box consensus sequence is AGCUUUA and for K box is UGUGAU. A search for microRNA recognition sites using miRBase revealed three potential microRNA binding sites within intron 7, with E values below 10, that suggests that these sites are active. The microRNAs hsa-miR-3118, hsa-miR-3976, and hsa-miR-5580-3p all have complementary bases to the *SMN* intron 7 sequence within the seed region. It is therefore possible that these microRNAs or the BRD and K box motifs could disrupt SMN translation.

The exon/intron 7-*SMN* transcript was further analyzed for polyadenylation [poly(A)] signals using two online tools, Polyadq[29] and DNA FS Miner.[30] Each tool identified two potential poly(A) sites with corresponding CA cleavage sites within intron 7. A potential poly(A)-1 (ATTAAA) signal was identified at 132 bases into intron 7, and a potential poly(A)-2 (AATAAA) signal was identified at 238 bases into intron 7. To determine whether early polyadenylation could destabilize the extended SMN transcript following PMO treatment, we designed specific poly(A) primers to target the predicted cleavage sites and downstream sequences to amplify polyadenylated products (Figure 5B). Following nucleofection of PMOs into unaffected fibroblasts, RNA was collected at multiple time points including 12, 24, 48, and 72 hr. Samples were DNase treated and RNA was amplified using the exon/intron 7 forward primer with the specific poly(A)-R1 and R2 primers (Figure 5C). No differences were observed within each treatment group over the 72-hr duration of the time course.

Specific poly(A)-R1 primer binding to the first ATTAAA poly(A) site amplified a faint product in some samples, suggesting this site could initiate polyadenylation. RT-PCR using the specific poly(A)-R2 primer directed to the second AATAAA site resulted in two products, a stronger amplicon amplified by the second cleavage site, as well as a fainter non-specific amplification of the first cleavage site. The stronger amplicon was sequenced and confirmed to have a poly(A) tail extending past the primer annealing site (Figure 5D). This result suggests that early polyadenylation is occurring at this second AATAAA site within intron 7, and as a result could destabilize the exon/intron 7-*SMN* transcript and therefore result in decreased protein levels.

To compare the stability and cleavage of the exon/intron 7-*SMN* and FL-*SMN* transcripts, we designed primers to target downstream of the poly(A) sites, and we tested them with a forward primer targeting the exon/intron 7 boundary (Figure 5C). Interestingly, both primer sets produce a strong amplicon extending beyond the poly(A) signal and do not show diminished expression of the transcript following AO treatment. Taken together, these results show that while early polyadenylation appears to occur at the second poly(A) signal, the transcript level remains stable, suggesting that transcription may be occur at a faster rate than polyadenylation and cleavage, or that the early polyadenylation is not destabilizing the transcript.

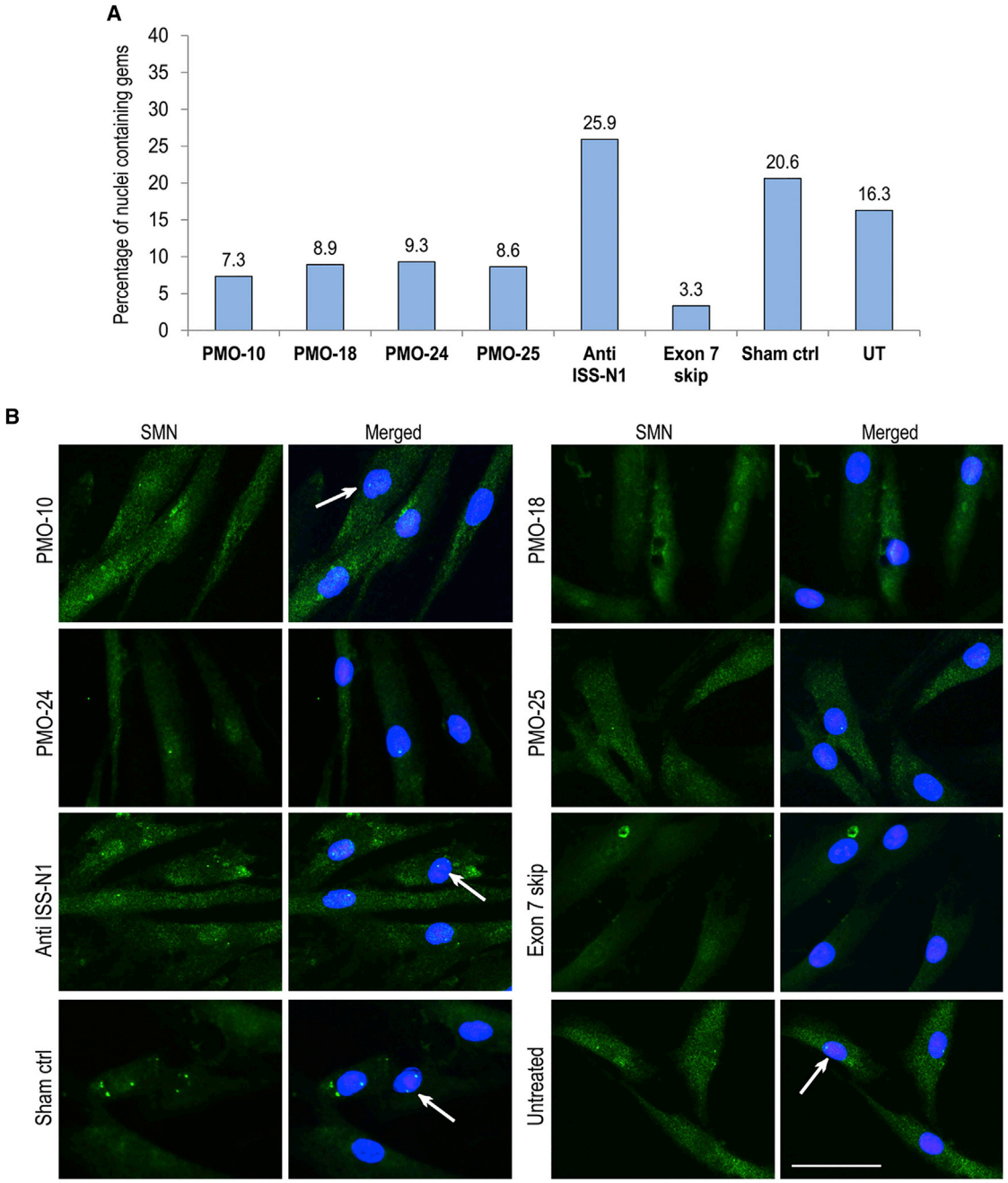


**Figure 4. Immunofluorescence Staining and Analysis of SMN Protein following PMO Nucleofection**

Immunofluorescence analysis of SMN shown as gems in PMO nucleofected unaffected fibroblasts (1 μM), compared with untreated fibroblasts. (A) Graph displaying the percentages of cell nuclei containing gems, as indicated above each bar, and (B) representative images showing anti-SMN- (green) and Hoechst (blue)-stained SMA fibroblasts following PMO nucleofection. Typical gems stained within the cell nucleus are indicated with white arrows. Images were taken at 20× objective. Scale bar, 25 μm.

## DISCUSSION

The original intent of this study was to influence the rate of *SMN2* transcription by targeting AOs to the terminal exon in an attempt to increase exon 7 inclusion. However, another splice-switching mechanism for manipulating expression was revealed. Selected AOs targeting *SMN2* exon 8 promoted exon 7 and intron 7 inclusion in the mature *SMN* message, revealing a novel AO application: inducing terminal intron retention. *In silico* analysis of the *SMN2* exon 7 splice sites suggests that this action may be the result of a strong acceptor splice site (scoring 98 out of 100) and a weaker donor splice site

**Table 2. *In Silico* Analysis of Potential Regulatory Elements within *SMN* Intron 7**

| Regulatory element | *SMN* recognition sequence | *SMN* intron 7 base location | Prediction value or score | Database |
|---|---|---|---|---|
| hsa-miR-3118 | 5′ UCUGCCAGCAUUAUGAAAGU 3′<br>3′ ACACUGACGUAAUACUUUUA 5′ | 4 | E-value 6.4 | miRBase |
| hsa-miR-3976 | 5′ UAGAAAGUUGAAAGGUUAAUGU 3′<br>3′ AUCUCUCGUCCUUCUAAUUACA 5′ | 96 | E-value 8.4 | miRBase |
| Poly(A) signal | ATTAAA | 132 | 0.000386 | Polyadq |
| | | | 0.566 | DNA FS miner |
| Poly(A) signal | AATAAA | 238 | 0.186149 | Polyadq |
| | | | 0.162 | DNA FS miner |
| BRD box | UAAAGCU | 245 | NA | UTRscan |
| K box | UAUCACA | 305 | NA | UTRscan |
| hsa-miR-5580-3p | 5′ ACAUAUGAAGUGCUCUAG 3′<br>3′ UGUAUACUUCACUCGGUC 5′ | 346 | E-value 7.7 | miRBase |

The prediction value or score indicates the strength of the regulatory site within the *SMN* sequence. For poly(A) signals, scores >0.5 are true predictions for Polyadq and scores >0.6 are true predictions for DNA FS Miner. For miRBase, E values <10 may have binding potential.
NA, not applicable.

(scoring 83 out of 100). The weaker donor site might be subject to poor recognition by the splicing machinery, abrogating splicing between exon 7 and the following exon, especially when the splicing of exon 8 is compromised by AO binding.

The correlation in splice-switching efficacy between 2′O-methyl and PMO compounds of the same sequence is well established for induced exon skipping in dystrophin transcripts as a therapy for Duchenne muscular dystrophy,[33] as well as for the efficacy of the *Anti-ISS-N1* sequence.[34] Furthermore, the PMO chemistry has been shown to be safe, with no significant adverse events reported in a 5-year study of Duchenne muscular dystrophy patients receiving weekly treatment with *Exondys51*, a PMO drug granted accelerated approval by the U.S. Food and Drug Administration (FDA) in 2016 for amenable dystrophin mutations.[35,36]

Consistent with the results of exon 8 targeting 2′O-methyl AOs, PMOs of the same sequence were effective at inducing exon/intron 7 retention. Interestingly, while PMOs targeting exon 8 increased the levels of the exon/intron 7-*SMN* transcript, these PMOs also induced a 50% decrease in SMN protein as assessed by western blot. This result was reproducible between SMA patient fibroblasts and unaffected fibroblasts following AO transfection. Similarly, immunofluorescence staining of the transfected fibroblasts showed fewer nuclei containing functional SMN in the form of "gems" when compared with sham-control PMO transfected cells. It is likely that the observed decrease in SMN protein could be due to the longer than normal 3′ UTR within the exon/intron 7-*SMN* transcript, and therefore many regulatory factors could contribute to protein downregulation.

Endogenous intron retention has been shown by others to act as a form of gene repression, often through the introduction of a premature termination codon, rendering the transcript susceptible to nonsense-mediated decay.[17,37] In the study presented here, nonsense-mediated decay is unlikely to be the cause of SMN downregulation due to the retained intron occurring after the normal termination codon. However, as a result of the extended 3′ UTR, influences of downstream sequences could lead to this transcript not being efficiently translated.

The length of the 3′ UTR can be a critical factor in regulating transcript stability and protein expression. A longer 3′ UTR can increase the opportunity for sequence-specific recognition motifs to recruit regulatory factors, including microRNAs.[16] Furthermore, the possibility of altered mRNA secondary structures can influence the availability of such sequences to these factors.[38] A number of online databases can identify potential microRNA and regulatory factor binding sites in NCBI documented transcripts. However, there is a lack of appropriate resources whereby an altered 3′ UTR sequence can be analyzed, limiting the search possibilities for this study. It is probable that there are many factors influencing the translational knockdown observed for the exon/intron 7-*SMN* transcript.

The microRNA prediction database miRBase allows the user to input an mRNA sequence for analysis, and analysis of the *SMN* intron 7 sequence revealed three potential microRNA binding sites. Of these, miR-3976 is a validated microRNA and is reportedly overexpressed in pancreatic cancer.[39] However, how miR-3976 impacts translation, and whether it is expressed in the dermal fibroblast used in this study, is yet to be determined. Further *in silico* analysis of the sequence using the online UTRscan database[27] drew attention to a number of motifs, including the BRD and K box motifs, as well as two alternative polyadenylation signals. The BRD box and K box motifs have been shown to recruit microRNAs that act as translational inhibitors of certain proteins during *Drosophila* development.[31,32,40] The functionality of these motifs in human sequences is unknown and, therefore, any influence on SMN translation is only speculative.

Others have tested the use of AOs to prevent microRNAs from binding to a transcript, by either binding of the microRNA as an antagomir, or to act as a decoy, binding directly to the transcript of interest.[41] To further investigate the mechanism of translational knockdown presented here, future studies could use AOs targeting the microRNAs themselves, their binding sites, as well as the BRD and K box motifs. Examining SMN expression in such studies could indicate whether these regulatory elements play a role in inhibiting SMN translation in the exon/intron 7-*SMN* transcript. However, it is unlikely that this will be of clinical benefit to SMA patients.

Further *in silico* analysis of the *SMN2* intron 7 sequence identified two potential polyadenylation signals with corresponding CA cleavage sites that could prematurely cleave the mRNA, potentially resulting in transcript and protein destabilization. Premature polyadenylation and mRNA cleavage have been shown by others to cause less efficient

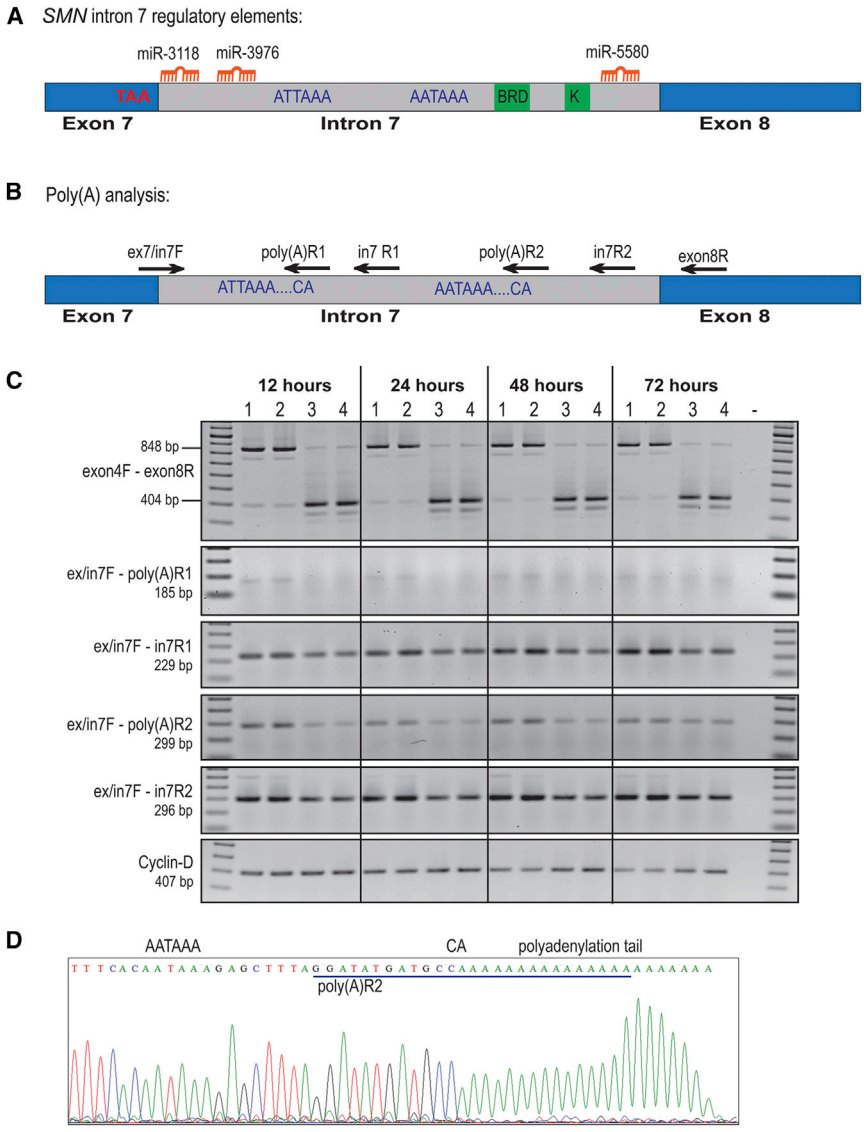


**Figure 5. Analysis of Predicted *SMN* Intron Regulatory Elements**

Analysis of predicted *SMN* intron 7 regulatory elements, showing (A) a schematic of the *in silico* analysis of regulatory elements within intron 7, (B) a schematic of the location of potential poly(A) signal and cleavage sites and the primer binding sites, (C) RT-PCR across *SMN* and *Cyclin-D* (housekeeping gene) transcripts in fibroblasts nucleofected with 1 μM (1) PMO-24, (2) PMO-25, (3) control PMO, and (4) an untreated sample, using indicated primers, and (D) sequencing chromatogram of the RT-PCR product amplified using the exon 6/7 forward and poly(A)R2 reverse primers.

processing of transcripts when compared with those cleaved at the distal 3′ or canonical poly(A) site.[42] In this study, primers were designed to anneal to the sites identified within intron 7, and should amplify a product only if polyadenylation has occurred. The primer designed to anneal to the ATTAAA site failed to generate a product, while the primer annealing to the AATAAA site amplified a clean, consistent product whose levels increased with an increase in intron 7 retention.

It appears that the early AATAAA site within intron 7 initiates polyadenylation prior to use of the canonical poly(A) site within exon 8, and as such negatively affects SMN translation. However, primers amplifying downstream of the early poly(A) site produced a strong and consistent product that is not diminished following AO treatment at any time point, indicating that mRNA cleavage does not occur downstream of either of the poly(A) signals. Taken together, these results show that while early polyadenylation appears to occur at the second poly(A) signal, the transcript level remains stable, suggesting that transcription in this case may occur at a faster rate than polyadenylation and cleavage.

Interestingly, the product amplified by the specific poly(A)-R2 primer was also observed in untreated samples, suggesting polyadenylation may be a natural mechanism for controlling SMN levels. Furthermore, it has been reported that the canonical poly(A) signal and cleavage site in *SMN* exon 8 is inefficient at recruiting cleavage factors, and consequently *SMN* polyadenylation is subjected to additional regulation by U1A, a component of the U1 snRNP.[43] The study showed that overexpression of U1A can inhibit *SMN* polyadenylation and cleavage, decreasing the levels of SMN protein.[43] Given the inefficiency of the canonical poly(A) site, it is probable that the intron 7 poly(A) signal could be more favorable for initiating polyadenylation and cleavage. However, the presence of U1A may still inhibit cleavage at this site, and therefore explain the lack of mRNA cleavage observed in the RT-PCR experiments within the current study.

The presence of polyadenylation signals in terminal introns could contribute to the process of protein regulation by intron retention. To examine this theory further, future studies should assess the occurrence of polyadenylation in alternatively spliced 3′ UTR-intron retention transcripts. It would be interesting to investigate whether this effect of "premature polyadenylation" occurs in other gene transcripts.

AOs targeting the terminal exon to induce intron retention could be useful in those diseases where protein repression is essential for treatment, including many types of cancer. We speculate that in the study

presented here, the extended SMN transcript is regulated by a number of motifs within intron 7 that are involved in translational repression due to the retention of this sequence in the 3′ UTR. However, this mechanism may only apply to a select number of genes. Alternatively, if the stop codon were to be in the final exon, intron retention could disrupt the reading frame or introduce a premature termination codon. To identify genes where intron retention could be applied, it will be necessary to look at a number of factors within the gene, most importantly the splice site scores for the flanking exons. If the donor site is strong, then intron retention may not be possible.

Aside from weakened splice sites of retained introns, additional *cis* and *trans* factors suggested to influence natural intron retention include the position of the intron in the transcript, an increase in G/C content, and reduced intron length.[17] Interestingly, while the G/C content of *SMN* intron 7 is only 33.8%, being positioned adjacent to an alternatively spliced exon increases the probability of the intron being retained. Furthermore, at 444 nt long, intron 7 is relatively short compared with the median human intron length of 1,334 nt in the coding region and 1,303 nt within the 3′ UTR.[44] It will be interesting in future studies to compare the relevance of these factors across transcripts to identify markers that could predict the likelihood of effective AO-induced intron retention.

In this study we present a novel application for splice-switching PMOs in initiating terminal intron retention. It is unfortunate that this model is unlikely to provide therapeutic benefit to SMA patients, yet further work could see intron retention being applied to a number of other diseases. This study is reflective of the ever-expanding complexity of gene regulation and undoubtedly sheds new light on splicing and AO mechanisms that may offer new avenues of therapy.

## MATERIALS AND METHODS

### AO Design and Synthesis

AOs were designed to target the exon 8 acceptor splice site and exon splice enhancers (ESEs) as predicted by the online SpliceAid prediction tool,[45] available at http://www.introni.it/splicing.html. AO nomenclature was based on that described by Mann et al.[46] All 2′O-methyl PS-AOs were synthesized in-house on an Expedite 8909 nucleic acid synthesizer with a phosphorothioate backbone. Following identification of optimal 2′O-methyl AO sequences, these AOs were prepared as PMOs, purchased through Genetools (Philomath, OR, USA). Table 3 lists the details of all AOs used in this study.

### 2′O-Methyl AO Transfection

SMA type I patient fibroblasts (GM03183; Coriell Cell Repositories, Camden, NJ, USA) and normal human dermal fibroblasts prepared in-house (Murdoch University Human Research Ethics Committee Approval #2013/156) were proliferated and seeded in 10% fetal bovine serum (FBS) DMEM and incubated at 37°C for 24 hr prior to transfection. All 2′O-methyl PS-AOs were transfected using Lipofectin (Life Technologies, Melbourne, Australia) at a 2:1 ratio of lipofectin to total AO, according to manufacturer's protocols, and incubated for 48 hr.

### Nucleofection of PMOs

PMO delivery by nucleofection was performed using a Nucleofection X unit with the Nucleofection P2 kit, using the CA-137 program (Lonza, Melbourne, Australia). PMOs were transfected at 1 and 0.5 μM, as determined by the final transfection volume, supplemented with 5% FBS DMEM and incubated for 72 hr.

### RNA Extraction and PCR

RNA was extracted using the MagMAX-96 Total RNA Isolation Kit, including a DNase treatment (Life Technologies), according to the manufacturer's instructions. RT-PCRs were performed using the One-Step SuperScript III RT-PCR kit with Platinum Taq Polymerase (Life Technologies) according to manufacturer's instructions. All primer sequences used in this study are detailed in Supplemental Materials and Methods. Products were amplified with the temperature profile, 55°C for 30 min, 94°C for 2 min, followed by 25–30 cycles of 94°C for 30 s, 56°C for 30 s, and 68°C for 1 min. Amplicon sequences were identified by Sanger sequencing at the Australian Genome Research Facility (AGRF, Perth, Australia).

### Western Blot Analysis

Cell lysates were prepared in 125 mM Tris/HCl (pH 6.8), 15% SDS, 10% glycerol (v/v), 1.25 μM PMSF (Sigma-Aldrich), protease inhibitor cocktail (3 μL/100 μL; P8340; Sigma-Aldrich), 0.004% bromophenol blue, and 2.5 mM dithiothreitol. Pellets were sonicated six times for 1-s pulses and samples denatured at 94°C for 5 min.

Approximately 10 μg of total protein (as determined by BCA assay) was loaded per sample on a NuPAGE Novex 4%–12% BIS/Tris gel (Life Technologies). Proteins were transferred onto a Pall Fluorotrans polyvinylidene fluoride (PVDF) membrane at 350 mA for 1 hr in western transfer buffer. MANSMA7 (1:1,000; Developmental Studies Hybridoma Bank) and β-tubulin (1:20,000; DSHB) monoclonal primary antibodies were incubated overnight at 4°C prior to detection using a Western Breeze Chemiluminescent Immunodetection System (Life Technologies), according to the manufacturer's instructions. Western blot images were captured on a Vilber Lourmat Fusion FX system using Fusion software, and Bio-1D software was used for densitometry analysis. All p values were calculated using a paired two-tailed t test, and SE bars were used to represent the SEM.

### Immunofluorescence

Cells on coverslips were fixed using ice-cold acetone-methanol (1:1), then blocked in 10% filtered goat serum in PBS containing 0.2% Triton-X (PBT). SMN was detected with MANSMA1 (1:100; DSHB) antibody, incubated overnight at 4°C in PBT. Cells were stained with Hoechst (Sigma-Aldrich) for nuclei detection (1 mg/mL diluted 1:125), and the MANSMA1 primary antibody was detected using Alexa Fluor 488 (1:400; Thermo Fisher Scientific). Photos were overlaid, and the number of gems per nuclei was counted

**Table 3. AO Sequences and *SMN1* and *SMN2* Binding Coordinates**

| Synthesis Round | AO Number | Annealing Coordinates | Sequence 5′ → 3′ | Length (bp) |
|---|---|---|---|---|
| 1: Initial screening | 1 | hSMN8A(−18+7) | GCA UUU CCU GCA AAU GAG AAA UUA G | 25 |
| | 2 | hSMN8A(−12+13) | AUG CCA GCA UUU CCU GCA AAU GAG A | 25 |
| | 3 | hSMN8A(−7+18) | GCU CUA UGC CAG CAU UUC CUG CAA A | 25 |
| | 4 | hSMN8A(−2+23) | GUG CUG CUC UAU GCC AGC AUU UCC U | 25 |
| | 5 | hSMN8A(+4+28) | AUU UAG UGC UGC UCU AUG CCA GCA U | 25 |
| | 6 | hSMN8A(+9+33) | GUG UCA UUU AGU GCU GCU CUA UGC C | 25 |
| | 7 | hSMN8A(+14+38) | UAG UGG UGU CAU UUA GUG CUG CUC U | 25 |
| | 8 | hSMN8A(+24+48) | AUC GUU UCU UUA GUG GUG UCA UUU A | 25 |
| | 9 | hSMN8A(+34+58) | GAU CUG UCU GAU CGU UUC UUU AGU G | 25 |
| | 10 | hSMN8A(+59+83) | AUC UUC UAU AAC GCU UCA CAU UCC A | 25 |
| | 11 | hSMN8A(+84+108) | AUA UUU UGA AGA AAU GAG GCC AGU U | 25 |
| | 12 | hSMN8A(+152+178) | CAU AAC UUU UAA UCA AGA AGA GUU ACC | 27 |
| | 13 | hSMN8A(+24+43) | UUC UUU AGU GGU GUC AUU UA | 20 |
| | 14 | hSMN8A(+44+63) | UUC CAG AUC UGU CUG AUC GU | 20 |
| | 15 | hSMN8A(+64+83) | AUC UUC UAU AAC GCU UCA CA | 20 |
| | 16 | hSMN8A(+29+48) | AUC GUU UCU UUA GUG GUG UC | 20 |
| | 17 | hSMN8A(+35+53) | GUC UGA UCG UUU CUU UAG UG | 20 |
| | 18 | hSMN8(+39+58) | GAU CUG UCU GAU CGU UUC UU | 20 |
| 2: Microwalking | 19 | hSMN8A(−12+18) | GCU CUA UGC CAG CAU UUC CUG CAA AUG AGA | 30 |
| | 20 | hSMN8A(−10+15) | CUA UGC CAG CAU UUC CUG CAA AUG | 24 |
| | 21 | hSMN8A(+39+63) | UUC CAG AUC UGU CUG AUC GUU UCU U | 25 |
| | 22 | hSMN8A(+44+68) | UCA CAU UCC AGA UCU GUC UGA UCG U | 25 |
| | 23 | hSMN8A(+55+79) | UCU AUA ACG CUU CAC AUU CCA GAU C | 25 |
| | 24 | hSMN8A(+57+81) | CUU CUA UAA CGC UUC ACA UUC CAG A | 25 |
| | 25 | hSMN8A(+59+78) | CUA UAA CGC UUC ACA UUC CA | 20 |
| Control AOs | ISS-N1 | hSMN2.7D(−10-29) | AUU CAC UUU CAU AAU GCU GG | 20 |
| | Skipping | mSmn7A(+7+36) | UGA GCA CUU UCC UUC UUU UUU AUU UUG UCU | 30 |
| | Sham | scrambled sequence | GCT ATT ACC TTA ACC CAG | 18 |

and recorded as a percentage of total nuclei, with at least 300 cells counted per slide.

### *In Silico* Analysis

A number of online databases were used to analyze the extended 3′ UTR sequence to identify potential regulatory elements. Splice site scores were analyzed by Human Splice Finder version 3.0 available at http://www.umd.be/HSF3/.[26] Regulatory element binding was predicted using UTR Scan available at http://itbtools.ba.itb.cnr.it/.[27] Polyadenylation signals were analyzed using Polyadq available at http://rulai.cshl.edu/tools/polyadq/polyadq_form.html[29] and DNA FS Miner available at http://dnafsminer.bic.nus.edu.sg/.[30]

## SUPPLEMENTAL INFORMATION

Supplemental Information includes Supplemental Materials and Methods and one figure and can be found with this article online at https://doi.org/10.1016/j.omtn.2018.01.011.

## AUTHOR CONTRIBUTIONS

Conceived and designed experiments: L.L.F., C.M., S.F., and S.D.W. Performed experiments: L.L.F., C.M., and I.L.P. Wrote and edited manuscript: L.L.F., C.M., I.L.P., S.F., and S.D.W.

## ACKNOWLEDGMENTS

The authors would like to acknowledge Project funding from the Parry Foundation, Spinal Muscular Atrophy Association of Australia, and the NHMRC (project grant 1086311). L.L.F. and I.L.P. received scholarships from Team Spencer and Muscular Dystrophy WA.

## REFERENCES

1. McAndrew, P.E., Parsons, D.W., Simard, L.R., Rochette, C., Ray, P.N., Mendell, J.R., Prior, T.W., and Burghes, A.H. (1997). Identification of proximal spinal muscular atrophy carriers and patients by analysis of SMNT and SMNC gene copy number. Am. J. Hum. Genet. *60*, 1411–1422.

2. Shababi, M., Lorson, C.L., and Rudnik-Schöneborn, S.S. (2014). Spinal muscular atrophy: a motor neuron disorder or a multi-organ disease? J. Anat. *224*, 15–28.

3. Lorson, C.L., Hahnen, E., Androphy, E.J., and Wirth, B. (1999). A single nucleotide in the SMN gene regulates splicing and is responsible for spinal muscular atrophy. Proc. Natl. Acad. Sci. USA *96*, 6307–6311.

4. Monani, U.R., Lorson, C.L., Parsons, D.W., Prior, T.W., Androphy, E.J., Burghes, A.H., and McPherson, J.D. (1999). A single nucleotide difference that alters splicing patterns distinguishes the SMA gene SMN1 from the copy gene SMN2. Hum. Mol. Genet. *8*, 1177–1183.

5. Porensky, P.N., and Burghes, A.H. (2013). Antisense oligonucleotides for the treatment of spinal muscular atrophy. Hum. Gene Ther. *24*, 489–498.

6. Chiriboga, C.A., Swoboda, K.J., Darras, B.T., Iannaccone, S.T., Montes, J., De Vivo, D.C., Norris, D.A., Bennett, C.F., and Bishop, K.M. (2016). Results from a phase 1 study of nusinersen (ISIS-SMN(Rx)) in children with spinal muscular atrophy. Neurology *86*, 890–897.

7. Finkel, R.S., Chiriboga, C.A., Vajsar, J., Day, J.W., Montes, J., De Vivo, D.C., Yamashita, M., Rigo, F., Hung, G., Schneider, E., et al. (2016). Treatment of infantile-onset spinal muscular atrophy with nusinersen: a phase 2, open-label, dose-escalation study. Lancet *388*, 3017–3026.

8. Singh, N.K., Singh, N.N., Androphy, E.J., and Singh, R.N. (2006). Splicing of a critical exon of human Survival Motor Neuron is regulated by a unique silencer element located in the last intron. Mol. Cell. Biol. *26*, 1333–1346.

9. U.S. Food and Drug Administration. (2016). FDA approves first drug for spinal muscular atrophy. December 23, 2016. https://www.fda.gov/NewsEvents/Newsroom/PressAnnouncements/ucm534611.htm.

10. Osman, E.Y., Miller, M.R., Robbins, K.L., Lombardi, A.M., Atkinson, A.K., Brehm, A.J., and Lorson, C.L. (2014). Morpholino antisense oligonucleotides targeting intronic repressor Element1 improve phenotype in SMA mouse models. Hum. Mol. Genet. *23*, 4832–4845.

11. Singh, N.N., Lawler, M.N., Ottesen, E.W., Upreti, D., Kaczynski, J.R., and Singh, R.N. (2013). An intronic structure enabled by a long-distance interaction serves as a novel target for splicing correction in spinal muscular atrophy. Nucleic Acids Res. *41*, 8144–8165.

12. Hua, Y., Vickers, T.A., Okunola, H.L., Bennett, C.F., and Krainer, A.R. (2008). Antisense masking of an hnRNP A1/A2 intronic splicing silencer corrects SMN2 splicing in transgenic mice. Am. J. Hum. Genet. *82*, 834–848.

13. Fong, N., Kim, H., Zhou, Y., Ji, X., Qiu, J., Saldi, T., Diener, K., Jones, K., Fu, X.D., and Bentley, D.L. (2014). Pre-mRNA splicing is facilitated by an optimal RNA polymerase II elongation rate. Genes Dev. *28*, 2663–2676.

14. Dujardin, G., Lafaille, C., de la Mata, M., Marasco, L.E., Muñoz, M.J., Le Jossic-Corcos, C., Corcos, L., and Kornblihtt, A.R. (2014). How slow RNA polymerase II elongation favors alternative exon skipping. Mol. Cell *54*, 683–690.

15. Lim, S.R., and Hertel, K.J. (2001). Modulation of survival motor neuron pre-mRNA splicing by inhibition of alternative 3′ splice site pairing. J. Biol. Chem. *276*, 45476–45483.

16. Barrett, L.W., Fletcher, S., and Wilton, S.D. (2012). Regulation of eukaryotic gene expression by the untranslated gene regions and other non-coding elements. Cell. Mol. Life Sci. *69*, 3613–3634.

17. Braunschweig, U., Barbosa-Morais, N.L., Pan, Q., Nachman, E.N., Alipanahi, B., Gonatopoulos-Pournatzis, T., Frey, B., Irimia, M., and Blencowe, B.J. (2014). Widespread intron retention in mammals functionally tunes transcriptomes. Genome Res. *24*, 1774–1786.

18. Bicknell, A.A., Cenik, C., Chua, H.N., Roth, F.P., and Moore, M.J. (2012). Introns in UTRs: why we should stop ignoring them. BioEssays *34*, 1025–1034.

19. Jaillon, O., Bouhouche, K., Gout, J.F., Aury, J.M., Noel, B., Saudemont, B., Nowacki, M., Serrano, V., Porcel, B.M., Ségurens, B., et al. (2008). Translational control of intron splicing in eukaryotes. Nature *451*, 359–362.

20. Ge, Y., and Porse, B.T. (2014). The functional consequences of intron retention: alternative splicing coupled to NMD as a regulator of gene expression. BioEssays *36*, 236–243.

21. Yap, K., Lim, Z.Q., Khandelia, P., Friedman, B., and Makeyev, E.V. (2012). Coordinated regulation of neuronal mRNA steady-state levels through developmentally controlled intron retention. Genes Dev. *26*, 1209–1223.

22. Wong, J.J., Ritchie, W., Ebner, O.A., Selbach, M., Wong, J.W., Huang, Y., Gao, D., Pinello, N., Gonzalez, M., Baidya, K., et al. (2013). Orchestrated intron retention regulates normal granulocyte differentiation. Cell *154*, 583–595.

23. Ni, J.Z., Grate, L., Donohue, J.P., Preston, C., Nobida, N., O'Brien, G., Shiue, L., Clark, T.A., Blume, J.E., and Ares, M., Jr. (2007). Ultraconserved elements are associated with homeostatic control of splicing regulators by alternative splicing and nonsense-mediated decay. Genes Dev. *21*, 708–718.

24. Bergeron, D., Pal, G., Beaulieu, Y.B., Chabot, B., and Bachand, F. (2015). Regulated intron retention and nuclear pre-mRNA decay contribute to PABPN1 autoregulation. Mol. Cell. Biol. *35*, 2503–2517.

25. Wong, J.J., Gao, D., Nguyen, T.V., Kwok, C.T., van Geldermalsen, M., Middleton, R., Pinello, N., Thoeng, A., Nagarajah, R., Holst, J., et al. (2017). Intron retention is regulated by altered MeCP2-mediated splicing factor recruitment. Nat. Commun. *8*, 15134.

26. Desmet, F.O., Hamroun, D., Lalande, M., Collod-Béroud, G., Claustres, M., and Béroud, C. (2009). Human Splicing Finder: an online bioinformatics tool to predict splicing signals. Nucleic Acids Res. *37*, e67.

27. Grillo, G., Turi, A., Licciulli, F., Mignone, F., Liuni, S., Banfi, S., Gennarino, V.A., Horner, D.S., Pavesi, G., Picardi, E., and Pesole, G. (2010). UTRdb and UTRsite (RELEASE 2010): a collection of sequences and regulatory motifs of the untranslated regions of eukaryotic mRNAs. Nucleic Acids Res. *38*, D75–D80.

28. Kozomara, A., and Griffiths-Jones, S. (2014). miRBase: annotating high confidence microRNAs using deep sequencing data. Nucleic Acids Res. *42*, D68–D73.

29. Tabaska, J.E., and Zhang, M.Q. (1999). Detection of polyadenylation signals in human DNA sequences. Gene *231*, 77–86.

30. Liu, H., Han, H., Li, J., and Wong, L. (2005). DNAFSMiner: a web-based software toolbox to recognize two types of functional sites in DNA sequences. Bioinformatics *21*, 671–673.

31. Lai, E.C., and Posakony, J.W. (1997). The Bearded box, a novel 3′ UTR sequence motif, mediates negative post-transcriptional regulation of Bearded and Enhancer of split Complex gene expression. Development *124*, 4847–4856.

32. Lai, E.C., Burks, C., and Posakony, J.W. (1998). The K box, a conserved 3′ UTR sequence motif, negatively regulates accumulation of enhancer of split complex transcripts. Development *125*, 4077–4088.

33. Adams, A.M., Harding, P.L., Iversen, P.L., Coleman, C., Fletcher, S., and Wilton, S.D. (2007). Antisense oligonucleotide induced exon skipping and the dystrophin gene transcript: cocktails and chemistries. BMC Mol. Biol. *8*, 57.

34. Mitrpant, C., Porensky, P., Zhou, H., Price, L., Muntoni, F., Fletcher, S., Wilton, S.D., and Burghes, A.H. (2013). Improved antisense oligonucleotide design to suppress aberrant SMN2 gene transcript processing: towards a treatment for spinal muscular atrophy. PLoS ONE *8*, e62114.

35. Mendell, J.R., Goemans, N., Lowes, L.P., Alfano, L.N., Berry, K., Shao, J., Kaye, E.M., and Mercuri, E.; Eteplirsen Study Group and Telethon Foundation DMD Italian Network (2016). Longitudinal effect of eteplirsen vs. historical control on ambulation in DMD. Ann. Neurol. *79*, 257–271.

36. U.S. Food and Drug Administration. (2016). FDA News Release: FDA grants accelerated approval to first drug for Duchenne muscular dystrophy. September 19, 2016. http://www.fda.gov/NewsEvents/Newsroom/PressAnnouncements/ucm521263.htm.

37. Aartsma-Rus, A., Bremmer-Bout, M., Janson, A.A., den Dunnen, J.T., van Ommen, G.J., and van Deutekom, J.C. (2002). Targeted exon skipping as a potential gene correction therapy for Duchenne muscular dystrophy. Neuromuscul. Disord. *12* (*Suppl 1*), S71–S77.

38. Chen, J.M., Férec, C., and Cooper, D.N. (2006). A systematic analysis of disease-associated variants in the 3′ regulatory regions of human protein-coding genes II: the importance of mRNA secondary structure in assessing the functionality of 3′ UTR variants. Hum. Genet. *120*, 301–333.

39. Madhavan, B., Yue, S., Galli, U., Rana, S., Gross, W., Müller, M., Giese, N.A., Kalthoff, H., Becker, T., Büchler, M.W., and Zöller, M. (2015). Combined evaluation of a panel

of protein and miRNA serum-exosome biomarkers for pancreatic cancer diagnosis increases sensitivity and specificity. Int. J. Cancer *136*, 2616–2627.

40. Lai, E.C. (2002). Micro RNAs are complementary to 3′ UTR sequence motifs that mediate negative post-transcriptional regulation. Nat. Genet. *30*, 363–364.

41. Beg, M.S., Brenner, A.J., Sachdev, J., Borad, M., Kang, Y.K., Stoudemire, J., Smith, S., Bader, A.G., Kim, S., and Hong, D.S. (2017). Phase I study of MRX34, a liposomal miR-34a mimic, administered twice weekly in patients with advanced solid tumors. Invest New Drugs *35*, 180–188.

42. Beaudoing, E., Freier, S., Wyatt, J.R., Claverie, J.M., and Gautheret, D. (2000). Patterns of variant polyadenylation signal usage in human genes. Genome Res. *10*, 1001–1010.

43. Workman, E., Veith, A., and Battle, D.J. (2014). U1A regulates 3′ processing of the survival motor neuron mRNA. J. Biol. Chem. *289*, 3703–3712.

44. Hong, X., Scofield, D.G., and Lynch, M. (2006). Intron size, abundance, and distribution within untranslated regions of genes. Mol. Biol. Evol. *23*, 2392–2404.

45. Piva, F., Giulietti, M., Burini, A.B., and Principato, G. (2012). SpliceAid 2: a database of human splicing factors expression data and RNA target motifs. Hum. Mutat. *33*, 81–85.

46. Mann, C.J., Honeyman, K., McClorey, G., Fletcher, S., and Wilton, S.D. (2002). Improved antisense oligonucleotide induced exon skipping in the mdx mouse model of muscular dystrophy. J. Gene Med. *4*, 644–654.